9-30-2016

Reduced Mechanism Validation and Analysis Near Extinction Limits of Perfectly Stirred Reactors

Brian J. Magda
brian.j.magda@gmail.com

Reduced Mechanism Validation and Analysis Near Extinction Limits of Perfectly Stirred Reactors

Brian Magda

B.S., University of Connecticut, 2014

A Thesis

Submitted in Partial Fulfillment of the

Requirements for the Degree of

Master of Science

At the

University of Connecticut

2016

Approval Page

Masters of Science

Reduced Mechanism Validation and Analysis Near Extinction Limits of Perfectly Stirred Reactors

Presented by

Brian Magda, B.S.

Major Advisor _____

Dr. Tianfeng Lu

Associate Advisor _____

Dr. Xinyu Zhao

Associate Advisor _____

Dr. Baki Cetegen

University of Connecticut

2016

Acknowledgements

I would like to thank Dr. Lu for supporting my research endeavors and being a great mentor. His patience and guidance has taught me much more than can be expressed on this piece of paper and will continuously shape what I do long after school.

I would like to thank my labmates for leading me and setting an example of what to strive for. I would particularly like to thank Yang Gao, Yufeng Liu, and Yunchao Wu. Without their patience and knowledge none of this would be possible. I would like to thank Dr. Ruiqin Shan for the help understanding code and difficult concepts and her previous work makes this thesis possible. I'd like to thank all my classmates who made me smile and gave me support throughout my time as student. Lenny, Steve, John, Nick, Briana, Guilio, Emily and everyone else, you are great. I would like thank my roommate Justin Bunnell for always being there to bounce idea off of. Over the last 5 years nobody has taught me more than he did.

I would like to thank UConn's Mechanical Engineering Department. I've been blessed to learn from such an array of professionals who were genuinely interested in cultivating knowledge. Also thanks to everyone from the ME office, all the kindness and help received goes a long way for a stressed out college student.

I'd like to thank my family and friends for always pushing me to do better and supporting me when I fail. Ultimately I am who I am today because of them and I can't thank them enough.

This work was supported by the Federal Aviation Administration under Grant 13-C-AJFE-GIT-009 and by the National Aeronautics and Space Administration under Grant NNX15AU96A.

Table of Contents

Abstract

Reduced mechanisms for jet fuels, including POSF10264, POSF10325, POSF10289, and n-dodecane as a surrogate, are extensively validated and investigated in perfectly stirred reactors (PSR). The ability of the reduced models to capture extinction limits and the important reaction pathways controlling the limit phenomena are investigated using a bifurcation analysis. In particular, extinction at conditions relevant to lean blow out (LBO) in jet engines is investigated.

It was found that the reduced models perform well over various equivalence ratios, pressures, and temperatures and can accurately capture extinction in PSR. The four jet fuels exhibited similar controlling reaction pathways, which involve only small molecules such as H, OH, HO_2, and CO, at LBO conditions based on the results from the bifurcation analysis. The controlling reaction pathways for extinction were found to be sensitive to pressure and equivalence ratio, while the four jet fuels show nearly identical “S”-curve response near the extinction conditions. The four fuels showed nearly identical LBO performance in a PSR and thus it is likely that any large differences in LBO performance of the fuels in

diffusive environments can be primarily attributed to the differences in their physical properties, such as diffusivity, viscosity and boiling point.

Chapter 1. Introduction

1.1. Background

The increasing demand and limited resources of traditional fossil fuels have propelled interest in the development of alternative energy sources. In 2014, 95% of the transportation sector's energy usage was derived from fossil fuels with a substantial contribution from aerospace (9%), which is projected to increase further in the future [1]. "Drop-in" alternative fuels are needed to eliminate costly alterations to existing engines. As an example, the Department of Defense has started the Assured Fuel Initiative to eliminate the nation's dependence on foreign oil aiming at domestically deriving half of the military aviation fuel from alternative sources by 2016, and have completed a test flight of a B-52 on a mix of conventional and alternative fuels [2].

Flame characteristics and chemical kinetics of alternative fuels and their surrogates have been extensively investigated. For instance, Hui et al. [3] conducted experiments with synthetic paraffinic kerosene fuels and hydrotreated renewable jet fuels to obtain their auto-ignition responses, laminar flame speeds, and extinction strain rates. Kumar et al. [4], [5] used a Rapid Compression Machine and a counterflow twin flame configuration to experimentally investigate auto-ignition characteristics, laminar flame speed and extinction stretch rate for a conventional jet fuel (Jet-A) and an alternative jet fuel (S-8). Ahmed et al. [6] performed experimental and numerical studies on synthetic jet fuels in a jet-stirred reactor and constructed a chemical kinetic model for 50:50 mixtures of synthetic and

commercial jet fuels. Valco et al. [7] investigated the auto-ignition characteristics and the effect of chemical composition of traditional military aviation fuels and renewable jet fuel replacements on auto-ignition in a RCM at low to intermediate temperatures.

The recent National Jet Fuels Combustion Program (NJFCP) copes with the challenge in streamlining the certification of alternative jet fuels by developing a generic yet rigorous fuel evaluation method facilitated by kinetic modeling and computational fluid dynamic (CFD) simulations [8]. The composition, chemical kinetics, and physical properties of current and alternative fuels, and their effects on engine performance will be investigated to provide information toward creating reliable modeling and design tools for industrial applications [9].

The development of high fidelity models of the combustion processes in engines requires accurate chemical kinetic mechanisms. However, due to the large number of fuel components and intermediate species formed during the pyrolysis and oxidation processes, creating comprehensive kinetic mechanisms for real jet fuels by including all important species and reaction pathways is a highly challenging task [10]. In addition, the large sizes render detailed mechanisms of real jet fuels unaffordable for CFD simulations, and thus the creation of robust and accurate reduced kinetic mechanisms is important for high fidelity CFD simulations of jet fuel combustion.

Reduced mechanisms of a variety of fuels have been developed in previous studies, and many methods have been developed for mechanism reduction. For

instance, Lu et al. [11] developed the method of directed relation graph (DRG), which features linear reduction time for constructing skeletal mechanisms. Sensitivity analyses have also been used to create skeletal mechanisms [12] which is computational expensive when the mechanisms are large. Zheng et al. [13] reduced the computational cost of sensitivity analysis using DRG aided sensitivity analysis (DRGASA). Lam and Goussis [14] developed the computational singular perturbation (CSP) theory that accurately separates the slow and fast chemical processes, such that exhausted fast processes can be approximated by algebraic equations. Lu et al. [15] used CSP to further develop a criterion for identifying quasi-steady state (QSS) species, which can be eliminated from the transport equations.

The ability of a reduced mechanism to capture both ignition and extinction chemistry is crucial for predicting limit phenomena in jet fuel combustion, such as lean blow out (LBO), ground starting and high-altitude relight. LBO and loss of thrust for an operating aircraft poses a significant safety threat while high-altitude relight are crucial to recovery of engine combustion. LBO and ignition relight are also strongly affected by fuel property variation [16]. Therefore, a systematic way to identify the processes controlling limit flame phenomena, such as ignition and extinction, is critical for developing and validating chemical kinetic mechanisms for jet fuel applications.

In the diagnostics of numerical and experimental datasets, scalars such as temperature and individual species concentrations are frequently used to identify

critical flame features [17], however expert knowledge and arbitrary thresholds are often required [18]. For large datasets generated from large scale simulations, e.g. the peta-scale direct numerical simulations (DNS) at Sandia National Laboratories [19], frequent human interaction is typically infeasible for systematic computation diagnostics of the massive datasets. To address this challenge, chemical explosive mode analysis (CEMA) [20] and bifurcation analysis [21] were developed to systematically detect critical flame features in different flames.

In particular, the bifurcation analysis was first applied in steady state combustion systems that feature the "S"-curve response. The turning points on the "S"-curves are widely accepted as ignition or extinction states of steady state systems. However, it was found in Ref. [21] that extinction can occur before reaching the turning points, and flame stability analysis is required to detect flame extinction in such cases [22]. Furthermore, Shan et al. [23] developed a method to identify the reactions controlling the bifurcation points and the method will be employed in the present study to determine important reaction pathways in jet fuel combustion at near-LBO conditions. PSR will be the primary system employed in the study at conditions relevant to LBO. Davis et al. [24] used a PSR to investigate flammability limits of cavity flame holders in a scramjet. Sigfrid et al. [25] used a network of PSRs in series to study the LBO of industrial swirl stabilized burners. PSR theory has also been useful in modeling flame recirculation zones of a combustor [26]. However, it is noted that PSR is a homogeneous model and may not fully account for the effects in actual flame extinction involving mixing processes.

1.2. Goal of this Thesis

The goal of this thesis is to validate reduced mechanisms of POSF10325 and n-dodecane in PSR at near LBO conditions, identify the controlling chemical reactions and performance of jet fuels at LBO using the bifurcation analysis developed by Shan et al. [27], and investigate chemical and physical processes role on real world combustor performance.

1.3. Organization of this Thesis

The methodologies of the study are presented in Chapter 2. The validation of the reduced mechanisms at extinction of a PSR is shown in Section 3.1. Section 3.2 analyzes important reaction pathways at LBO in a PSR and determines the effects of operating conditions on the controlling reaction pathways. Section 3.3 compares the extinction behaviors of the different fuels. Chapter 4 summarizes the results from the study and indicates potential future work.

Chapter 2. Methodologies

As previously mentioned, the canonical "S"-curve is an important feature of steady state PSRs, and a typical "S"-curve is shown in Fig. 2.1. Note that, when negative temperature coefficient (NTC) behaviors and cool flames are involved the "S"-curves can consist of more branches as shown in [21]. The upper turning point on the conventional "S"-curve is accepted as the extinction state and the lower turning point as the ignition state. The middle branch of the "S"-curve (the dashed segment in Fig. 2.1) is physically unstable and its significance in practical systems merits further study. The turning points are bifurcation points that separate unstable middle branch from the stable branches and mathematically are associated with singular Jacobian [28]. It was further shown that additional bifurcation points may exist on the "S"-curves for practical fuels such as DME [23], and extinction may occur at these non-turning bifurcation points. Linear stability analysis was employed to determine locations of such bifurcation points and the underlying controlling processes by Shan et al. [22].

As a brief review of the bifurcation analysis, unsteady PSR will be used in the following and the governing equations are:

$$\frac{d\boldsymbol{y}}{dt} = \boldsymbol{g}(\boldsymbol{y}) = \boldsymbol{\omega}(\boldsymbol{y}) + \boldsymbol{s}(\boldsymbol{y}), \qquad \boldsymbol{y} = [Y_1, Y_2, \ldots . Y_k, T]^T \tag{2.1}$$

$$\omega_i(\boldsymbol{y}) = \frac{\dot{m}_i}{\rho}, i = 1,2, \ldots . K, \omega_{K+1}(\boldsymbol{y}) = -\sum_{i=1}^{K}\left(\frac{\dot{m}_i h_i}{\rho c_p}\right) \quad (2.2)$$

$$s_i(\boldsymbol{y}) = \frac{Y_i^0 - Y_i}{\tau}. i = 1,2, \ldots K, s_{K+1} = \frac{\sum_{i=1}^{K} Y_i^0 (h_i^0 - h_i)}{c_p \tau}, \tau = \frac{\rho V}{\dot{M}_{in}} \quad (2.3)$$

Where $\boldsymbol{y}$ is a vector of dependent variables, Y_i is the mass fraction of the *i*th species, and T is the temperature. Bold italic symbols represent vector quantities, bold script symbols represent matrices, and non-bold symbols represent scalar quantities. $\boldsymbol{\omega}$ represents the chemical source term while $\boldsymbol{s}$ represents the contribution from the inlet and outlet of the PSR and shall be referred to as the "mixing term" hereafter. $\dot{m}_i$ is the volumetric mass production rate of the *i*th species, ρ is the density, K is the number of species, h_i is the specific enthalpy of the *i*th species, c_p is the mixture-averaged specific heat, V is the volume of the reactor, τ is the residence time defined based on the inlet mass flow rate, $\dot{M}_{in}$. The super script "0" denotes the inlet conditions.

Stability of the system can be determined by inducing a small perturbation, $\boldsymbol{\delta y}$, and investigating the response of the system to the perturbation. Let $\boldsymbol{y_0}$ represent the steady state of the system, the growth of the perturbation can be linearly approximated as:

$$\frac{d(\boldsymbol{y_0} + \boldsymbol{\delta y})}{dt} = \boldsymbol{g}(\boldsymbol{y_0} + \boldsymbol{\delta y}) \approx \boldsymbol{g}(\boldsymbol{y_0}) + \mathbf{J_g}(\boldsymbol{y_0})\boldsymbol{\delta y} \quad (2.4)$$

$$\frac{d\boldsymbol{\delta y}}{dt} \approx \mathbf{J_g}(\boldsymbol{y_0})\boldsymbol{\delta y}, \qquad \mathbf{J_g} = \frac{d\boldsymbol{g}}{d\boldsymbol{y}^T} \tag{2.5}$$

Where $\mathbf{J_g}$ is the Jacobian evaluated at the steady state of the system. Using eigenvalue decomposition the perturbation growth can be expressed as

$$\mathbf{J_g} = \mathbf{A\Lambda B}, \qquad \frac{d\boldsymbol{\delta y}}{dt} = \mathbf{A\Lambda B}\boldsymbol{\delta y}, \qquad \mathbf{B} = \mathbf{A^{-1}} \tag{2.6}$$

$$\frac{d\boldsymbol{f}}{dt} = \mathbf{\Lambda}\boldsymbol{f}, \qquad \text{where } \boldsymbol{f} = \mathbf{B}\boldsymbol{\delta y} = \mathbf{A^{-1}\delta y} \tag{2.7}$$

$$f_i \approx f_{i_0} e^{\lambda_i t} \tag{2.8}$$

where **A** and **B** are matrices containing the right and left eigenvectors, respectively, **Λ** is a diagonal matrix containing the eigenvalues, λ_i represents the *i*th eigenvalue and f_{i_0} is an arbitrary constant. Based on Eq. 2.8, the presence of an eigenvalue with a positive real part will result in exponential growth of the perturbation and thus an unstable system. A system with all negative real parts of eigenvalues tends to relax toward the steady state when perturbed. Imaginary eigenvalues will lead to an oscillatory response but are not of the primary interest in this study.

For convenience, the "maximum" eigenvalue of the system λ_e is defined such that

$$e = \underset{i=\{1,2,\ldots K+1\}}{\arg\max} \left(Re(\lambda_i)\right) \tag{2.9}$$

$$\lambda_i = \boldsymbol{b_i} \mathbf{J_g} \boldsymbol{a_i} \tag{2.10}$$

where $Re(\,)$ denotes the real part of a number, arg max is the arguments of the maximum function, e is the index of the "maximum" eigenvalue, $\boldsymbol{b_i}$ and $\boldsymbol{a_i}$ are the left and right eigenvectors, respectively, associated with the eigenvalue λ_i. For $Re(\lambda_e) < 0$ the system is stable while for $Re(\lambda_e) > 0$ the system is unstable.

The Jacobian can be further decomposed to determine the contribution from each reaction and the mixing term:

$$\mathbf{J_g} = \sum_{r=1}^{II+1} \mathbf{J_r}\,, \qquad \mathbf{J_{II+1}} = \mathbf{J_s} \tag{2.11}$$

Where $\mathbf{J_r}$ represents the contribution to the full Jacobian from the *r*th reaction or the mixing term, and $\mathbf{J_s}$ is the contribution to the full Jacobian from the mixing term. II is the total number of reactions. The importance of each reaction and the mixing term at extinction can then be quantified by their contribution to the "maximum" eigenvalue.

$$\lambda_e = \boldsymbol{b_e} \mathbf{J} \boldsymbol{a_e} = \sum_{r=1}^{II+1} \boldsymbol{b_e} \mathbf{J_r} \boldsymbol{a_e} = \sum_{r=1}^{II+1} \lambda_r\,, \qquad \lambda_r = \boldsymbol{b_e} \mathbf{J_r} \boldsymbol{a_e} \tag{2.12}$$

Where $\lambda_r$is the contribution of each reaction or mixing term. A Bifurcation Index (BI) can be adopted from Shan et al. [22] to normalize individual contributions.

$$BI^r = \frac{Re(\lambda_r)}{\max\limits_{r=\{1,2..II+1\}}(|Re(\lambda_r)|)} \tag{2.13}$$

Only the real part's contribution is considered in the formulation of the bifurcation index because only the real part determines the stability. BI is normalized between the values of [-1, 1]. $|BI^r|$ close to unity represents important reactions for the bifurcation while BI^r close to zero represents relatively unimportant ones. Bifurcation index with opposing signs indicate competing processes.

The Jacobian in this study is calculated analytically using an in-house code to minimize numerical error and reduce computational cost. For more information the reader is directed to an extensive study on the performance and advantages of using an analytical Jacobian performed by Youssefi [29]. The detailed mechanisms for the fuels were developed by Prof. Hai Wang at Stanford University [30] and reduced using DRG, sensitivity analysis, Linearized QSSA [31] and validated by Yang Gao [32]. The reduction parameter range was the pressure from 0.5 to 30 atm, the equivalence ratio from 0.5 to 1.5, 1000 -1600 K as the initial temperature for auto-ignition, and 300 K as the inlet temperature for a PSR. A 20% error tolerance was used in sensitivity analysis on the target parameters of ignition delay and PSR extinction residence time. The mechanisms sizes are shown in Table 2.1.

Table 2.1 Mechanism Size	**Molecular Formula**	**Detailed Mechanism**		**Reduced Mechanism**	
		# Species	# Reactions	# Species	# Reactions
CAT A1 (POSF 10264)	$C_{11}H_{22}$	112	790	N/A	N/A
CAT A2 (POSF 10325)	$C_{11}H_{22}$	112	790	29	185
CAT A3 (POSF 10289)	$C_{12}H_{23}$	112	790	N/A	N/A
n-Dodecane [32][33]	$C_{12}H_{26}$	123	977	24	193

To further investigate the accuracy of the reduced mechanism over a wide range of equivalence ratios at near-LBO conditions, an additional mapping of the steady state solutions of a PSR was performed. That is to calculate the steady state solutions with varying equivalence ratio, resulting in the "O"-curves shown in Fig 2.2. NTC chemistry behavior can dramatically alter the shape of the curve but its effects are not pursued in this study. The "O"-curve consists of an unstable lower branch that is analogous to the unstable middle branch of the "S"-curve, and the turning points are identical to those on the "S"-curve. On the "O"-curve the leftmost turning point is the LBO limit while the rightmost turning point is the rich blow out (RBO) limit.

As observed in Fig 2.2, the turning points do not necessarily correspond to the physical extinction points. Instabilities on the upper branch show that RBO can occur prior to achieving the conditions at the right turning point. However the instabilities were only observed to occur on the upper branch only when the reactor was under conditions that could sustain an extremely rich flame ($\phi \approx 4.2$ in Fig 2.2). Reactors with high inlet temperatures or with long residence times are

examples of conditions necessary for sustaining an extremely rich flame and are not investigated in this study. Therefore for this study turning points are equivalent to extinction points and are the primary target of LBO analysis.

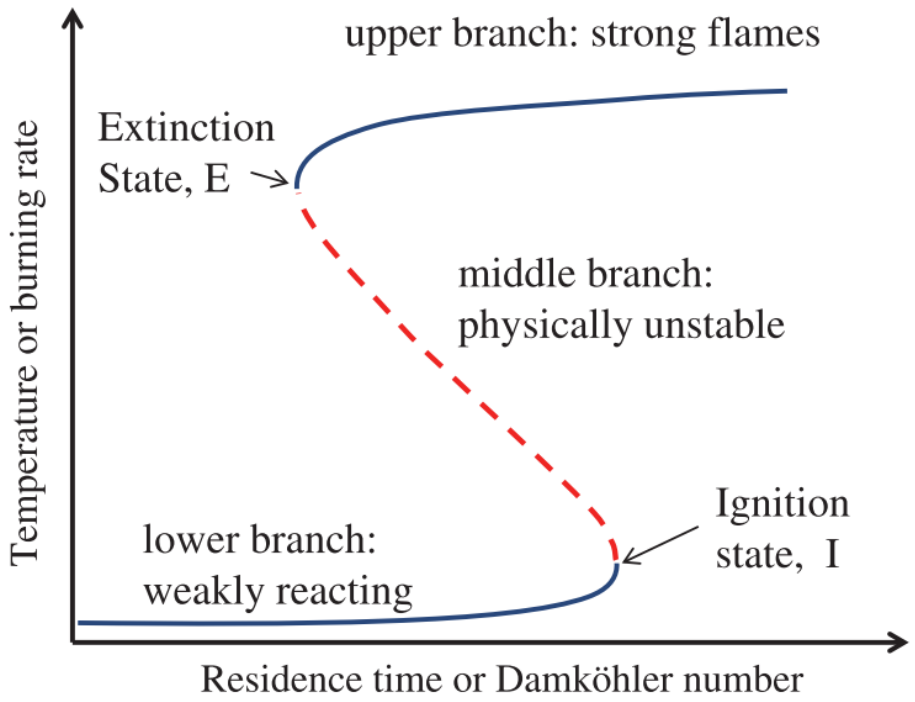

Figure 2.1 A canonical "S"-curve [17], the arrows pointing to the upper and lower turning points.

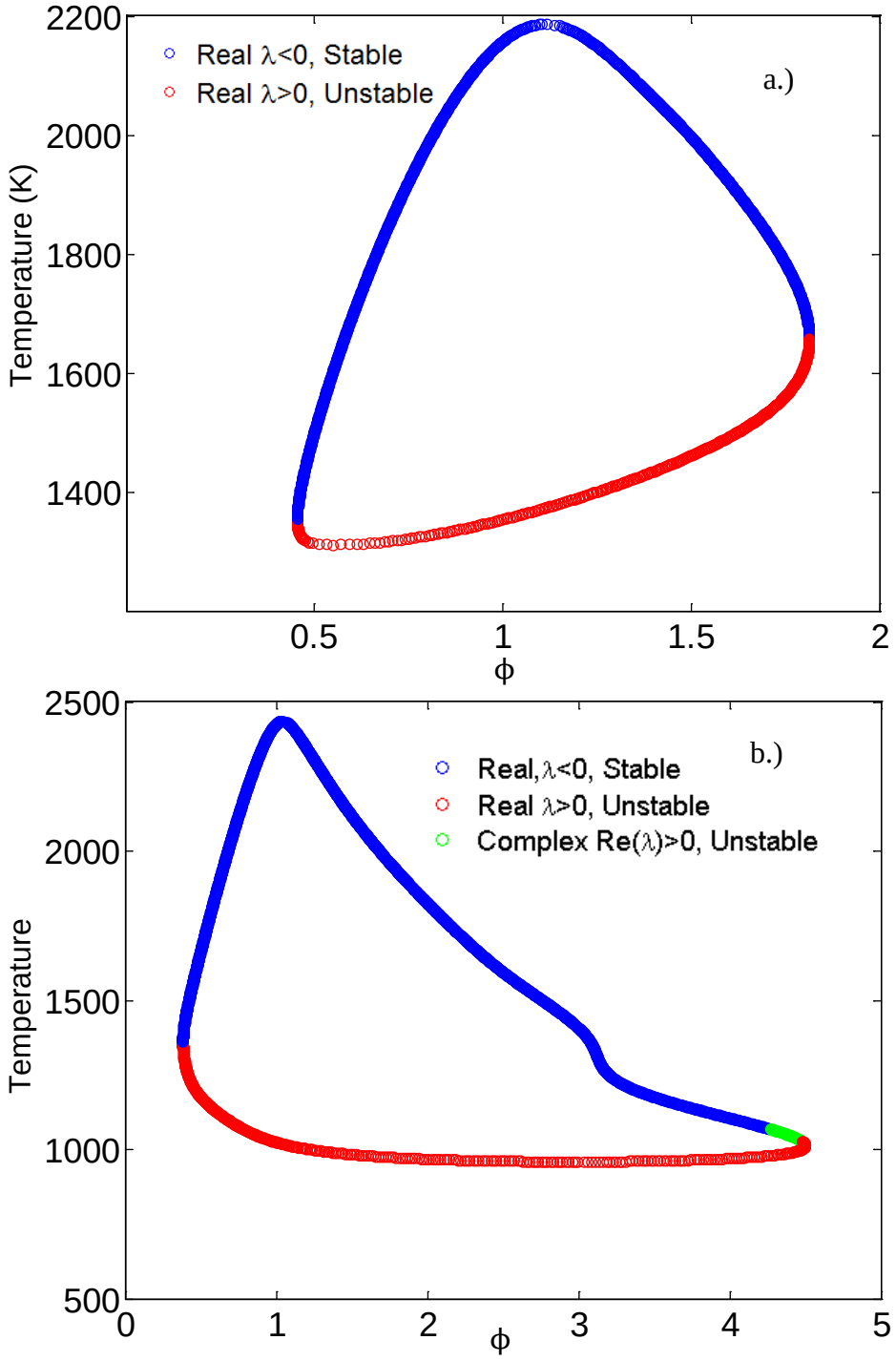

Figure 2.2 Temperature as a function of equivalence ratio for PSR at a) inlet temperature of 394 K, residence time of 1 ms and pressure of 2.04 atm and b) inlet temperature of 500 K, residence time of 5 ms, pressure of 10 atm.

Chapter 3. Results and Discussions

3.1. Validation of PSR extinction

The ability of reduced model to capture the extinctions state in a PSR has been tested extensively for equivalence ratio ranging from 0.5 to 1.5, pressure of 0.5 – 5 atm, and inlet temperature from 250 – 1000 K, which is relevant to jet fuel applications [34]. Extinction temperature and residence time predicted by the reduced model are compared with the detailed/lumped model for various inlet temperatures and pressures. The results for n-dodecane are shown in Figs 3.1 and 3.2, and those for POSF10325 are shown in Figs 3.3 and 3.4. Figure 3.4 demonstrates the effect of inlet temperature on extinction residence time. As the inlet temperature increases, the flame becomes more difficult to extinguish. Thus a higher inlet flowrate is required to extinguish the flame, as indicated by the decreased extinction residence time. It can be seen that the reduced mechanisms agree well with the detailed mechanisms. The maximum relative errors of the extinction residence time in the reduced models are about 19% for n-dodecane and 14% for POSF10325. The maximum errors of extinction temperature associated with the reduced models are about 44 K for n-dodecane and 22 K for POSF10325. It is noted that the error in the extinction residence time and temperature of the reduced models is rather small considering the uncertainties in the detailed models.

The reduced mechanisms were also validated for near-LBO conditions derived for PSR by Colket et al. [35], as shown in Table 3.1.

Table 3.1 Selected near-LBO conditions for PSR [35].

Conditions	T_{in}, K	P, atm	ϕ
Case 1	394	2.04	.457
Case 2	394	3.4	.456
Case 3	450	2.04	.435
Case 4	450	3.4	.434

The inlet conditions of PSR are fixed at 0.5 ms, 1 ms, and 2 ms for the flame conditions in Table 3. Figs 3.5 and 3.6 show the steady state solutions of a PSR as a function of equivalence ratio for n-dodecane/air and POSF10325/air respectively. It is seen that the reduced models and detailed models agree quite well, especially at LBO conditions. The maximum error appears in the lower branch and under rich conditions. The error in the lower branch is likely inconsequential towards developing an accurate model for practical systems as it is the physically unstable branch.

3.2. Reaction Pathway Analysis

The reaction pathways at the different LBO conditions used by Colket et al. [35] were investigated. Important reactions at LBO extinction were investigated using the Bifurcation Index (BI) discussed in Chapter 2. The analysis was performed using the detailed mechanism of each fuel. The BI results for n-dodecane and POSF10264 are shown in Fig 3.7 while those for POSF10325 and POSF10289 are shown in Fig 3.8. It is seen from that small molecule chemistry dominates the extinction process at LBO of the tested fuels. It is also observed that the chemical pathways at extinction remain relatively insensitive to the conditions in Table 3.1, including difference in residence times. It was found that the following four reactions have most significant effect on LBO.

Table 3.2 Important reactions at LBO identified using bifurcation analysis

Reaction		Sign of BI
R1	$H + O_2 (+M) \leftrightarrow HO_2 (+M)$	-
R2	$H + O_2 \leftrightarrow O + OH$	+
R3	$CO + OH \leftrightarrow CO_2 + H$	+
R4	$OH + OH (+M) \leftrightarrow H_2O_2 (+M)$	_

It is noted that the order of the reactions does not follow the particular order listed in Table 3.2 for all the fuels tested. Particularly the order of R2 and R3 changes

depending on the fuel type. As discussed in Chapter 2, different signs indicate opposite contribution to the bifurcation. It is seen that the hydrogen sub-chemistry plays an important role at LBO as evident by the importance of R1, R2, and R4.

The roles of R1 and R2 in hydrogen oxidation has been well studied, e.g. in affecting the second explosive limit [36]. In the absence of high pressure, HO_2 is a meta-stable species and thus R1 acts as a chain terminating reaction that impedes the branching of radicals. R4 is also a chain termination reaction and shares the same characteristics of R1. R2 and R3 are both favorable reactions for sustaining the flame, R2 is a chain branching reaction and R3 is an important exothermic reaction.

However, under higher pressures the stability of HO_2 is compromised such that R1 is no longer a chain termination reaction. The important reactions at LBO of n-dodecane at elevated pressure are shown in Fig 3.9. As it can be seen, R1 is no longer an important reaction pathway. R1's primary function of creating HO_2 no longer signifies a chain termination reaction at elevated pressures. The destruction of HO_2 now plays a greater role to facilitate the creation of H_2O which is a more stable species. Formation of H_2O is exothermic which releases heat and promotes increased reactivity but is also a chain terminating reaction that depletes the radical pool, which tends to reduce the reactivity. These competing factors can be seen in Fig 3.9 where the BI of reactions producing H_2O are both positive and negative. From Fig 3.9 it can be seen that reactions that produce H_2O and a radical have a positive BI (i.e. $OH + OH \leftrightarrow H_2O + O$) while reactions that are chain terminating

and produce H_2O have negative BI (i.e. $OH + HO_2 \leftrightarrow H_2O + O_2$). The heat release by H_2O formation appears to have little effect on the role of this reaction at LBO. Therefore it appears that radical proliferation plays an dominant role in sustaining the flame and preventing LBO.

The pressure dependence of important reactions for n-dodecane at extinction can also be seen in Fig 3.10. As can be seen in Fig 3.10, the stability of HO_2 seems to become compromised at a pressure of approximately 5 atm. The reaction pathways are primarily sensitive to pressure change within a pressure range of 5 - 19 atm. At pressure exceeding 19 atm the reactions' importance does not undergo any dramatic changes. It is because at this point pressure is elevated to such an extent that HO_2 is no longer stable, and further increasing pressure has little or no effect on changing the reaction pathways controlling extinction.

The effects of pressure on the extinction temperature and extinction equivalence ratio are shown in Fig 3.11. The minimum extinction equivalence ratio can be seen to occur around pressure of 2 atm. The location of this minimum signifies the optimal operating pressure of the PSR reactor for preventing LBO. However, due to the nature of the spatially homogeneous PSR model, physical properties of the fuels such as viscosity and diffusivity and their effects on mixing and flow patterns are not considered, and thus the optimal operating pressure shown in Fig 3.12 is strictly for chemical processes.

Reaction pathway sensitivity to inlet temperature was also analyzed. In Fig 3.12 it can be seen that inlet temperature has little to no effect on the important reaction

pathways for extinction. Fig 3.12 also contains extinction temperature and extinction equivalence ratio as a function of inlet temperature. It can be seen that the extinction equivalence ratio monotonically decreases with increasing inlet temperature, as the reactivity of the mixture increase with temperature and thus allowing for a stronger flame.

3.3. Flame Holding Capabilities

The flame holding capabilities of individual fuel in PSR were investigated to determine the effects the fuel's composition on LBO. Fig 3.13 shows the BI of important reactions at LBO for the four fuels tested. It is seen that the important reactions with significant BIs are similar for the different fuels at LBO conditions. The similarities in reaction pathways are favorable for the construction of a unified reduced mechanism for the different fuels. Fig 3.14 demonstrates the flame holding capabilities of each fuel. The intersection points of a drawn horizontal line and the curve represent the LBO limit and rich blow out (RBO) limit respectively for a specific residence time. It is shown from the figure that the four fuels investigated share almost identical LBO performance and slightly different RBO performance. It can be concluded that the differences in fuel composition of the fuels tested have little effect on the chemical processes that effect LBO performance.

Section 3.2 concluded that small molecular reactions are the most significant chemical reactions pathways at LBO. As oxidation of most hydrocarbon fuels involves the same foundation chemistry of small molecules, it appears that

chemical properties of individual fuels has little effect on LBO performance, and the physical properties of the fuels, such as viscosity and diffusivity, may play an important role in any fuel sensitivity of LBO. The importance of physical properties should also be considered when choosing and designing surrogate fuels for testing of LBO performance.

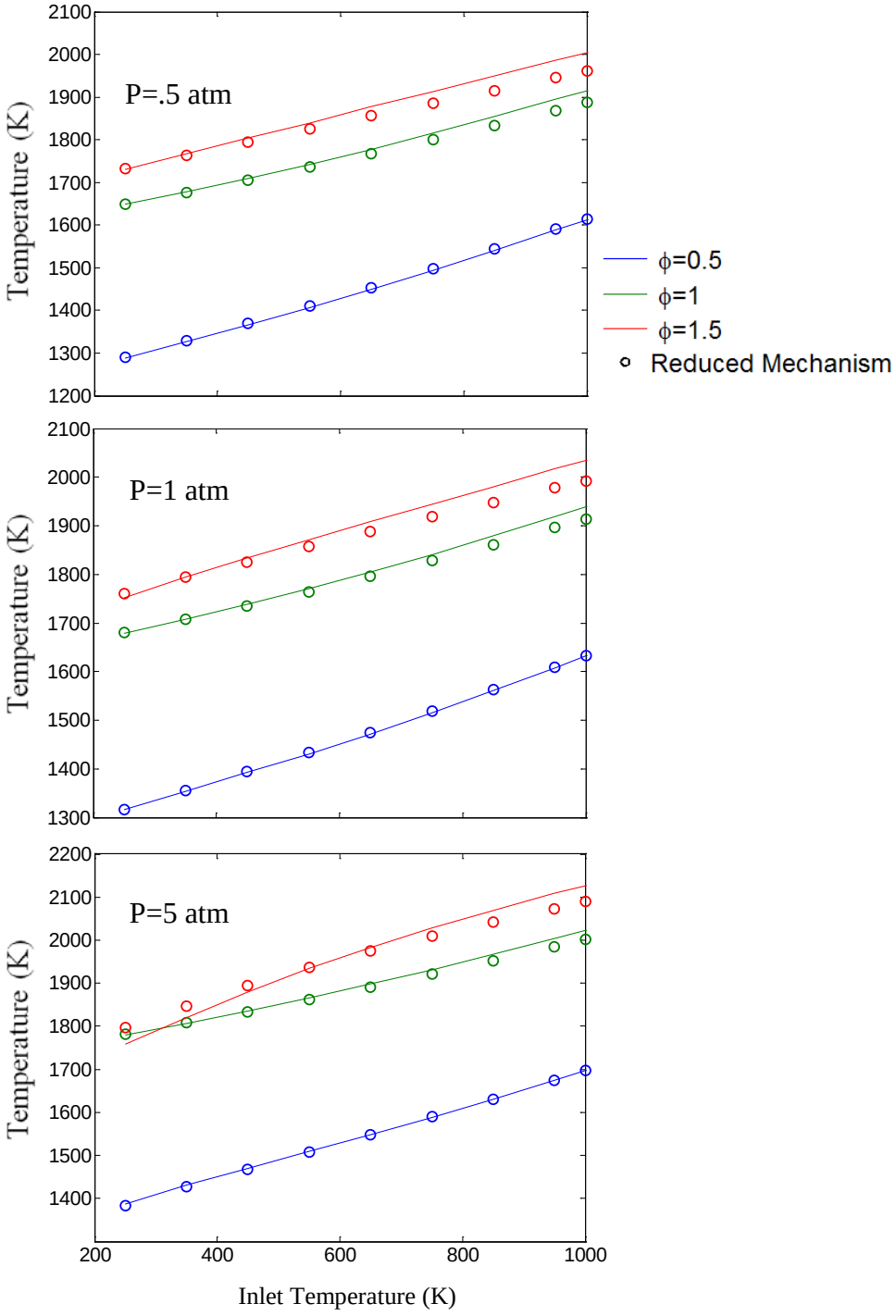

Figure 3.1 Extinction temperature in a PSR for n-dodecane/air as function of inlet temperature for different equivalence ratios and pressures. Lines: detailed/lumped mechanism, symbols: reduced mechanism.

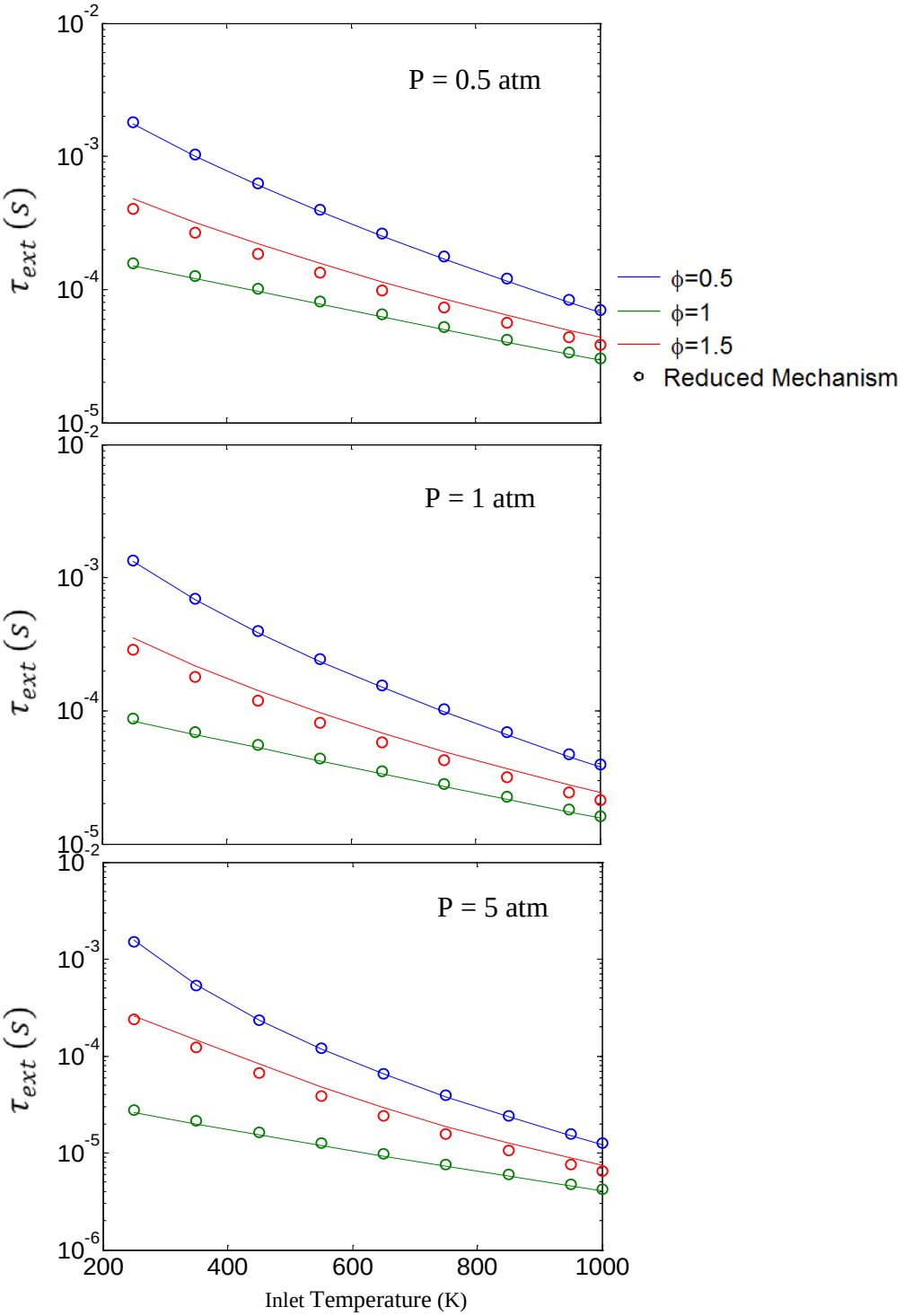

Figure 3.2 Extinction residence time of PSR for n-dodecane/air as function of inlet temperature for different equivalence ratios and pressures. Lines: detailed/lumped mechanism, symbols: reduced mechanism.

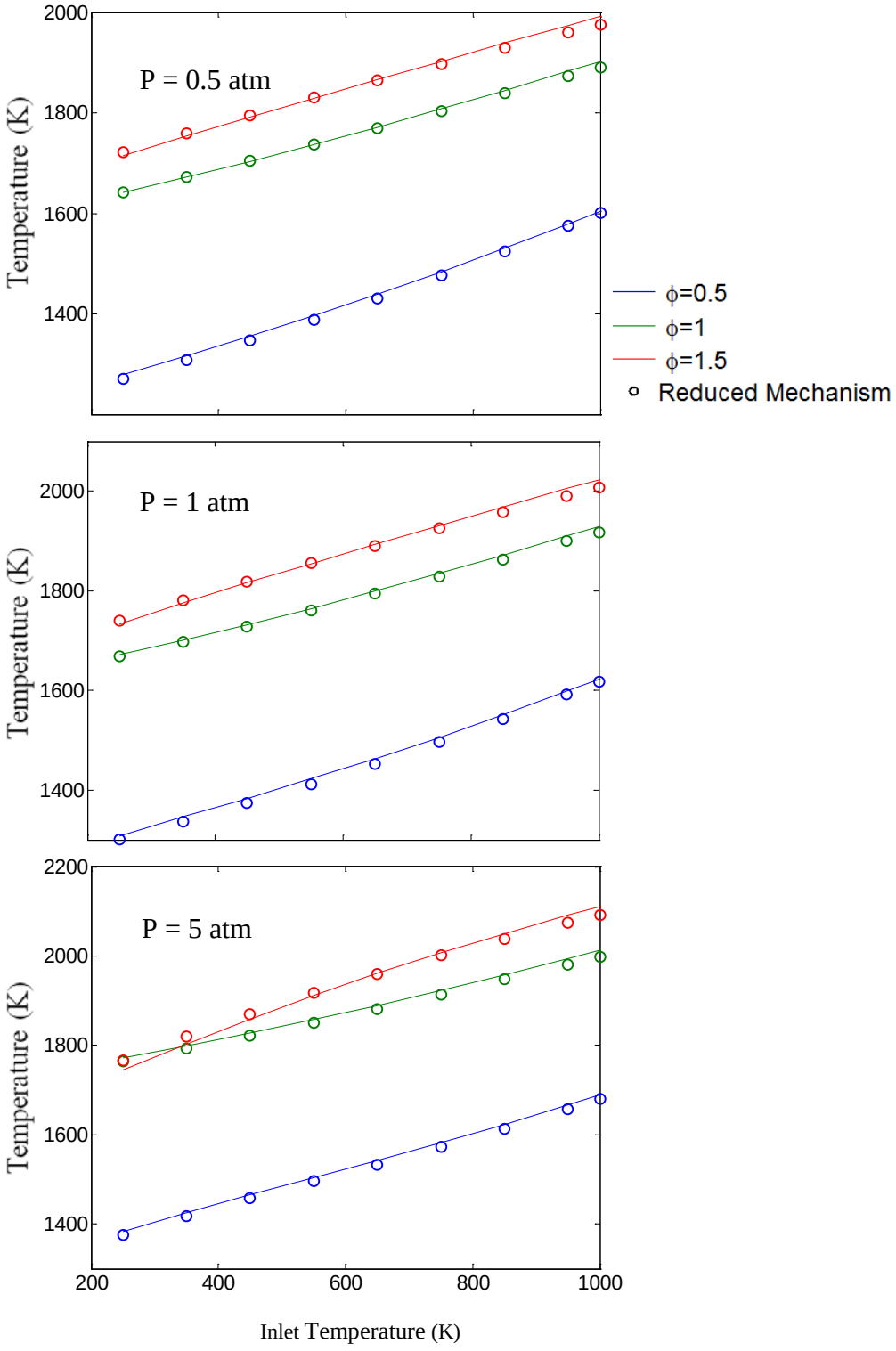

Figure 3.3 Extinction temperature in a PSR for POSF 10325 as function of inlet temperature for different equivalence ratios and pressures. Lines: detailed/lumped mechanism, symbols: reduced mechanism.

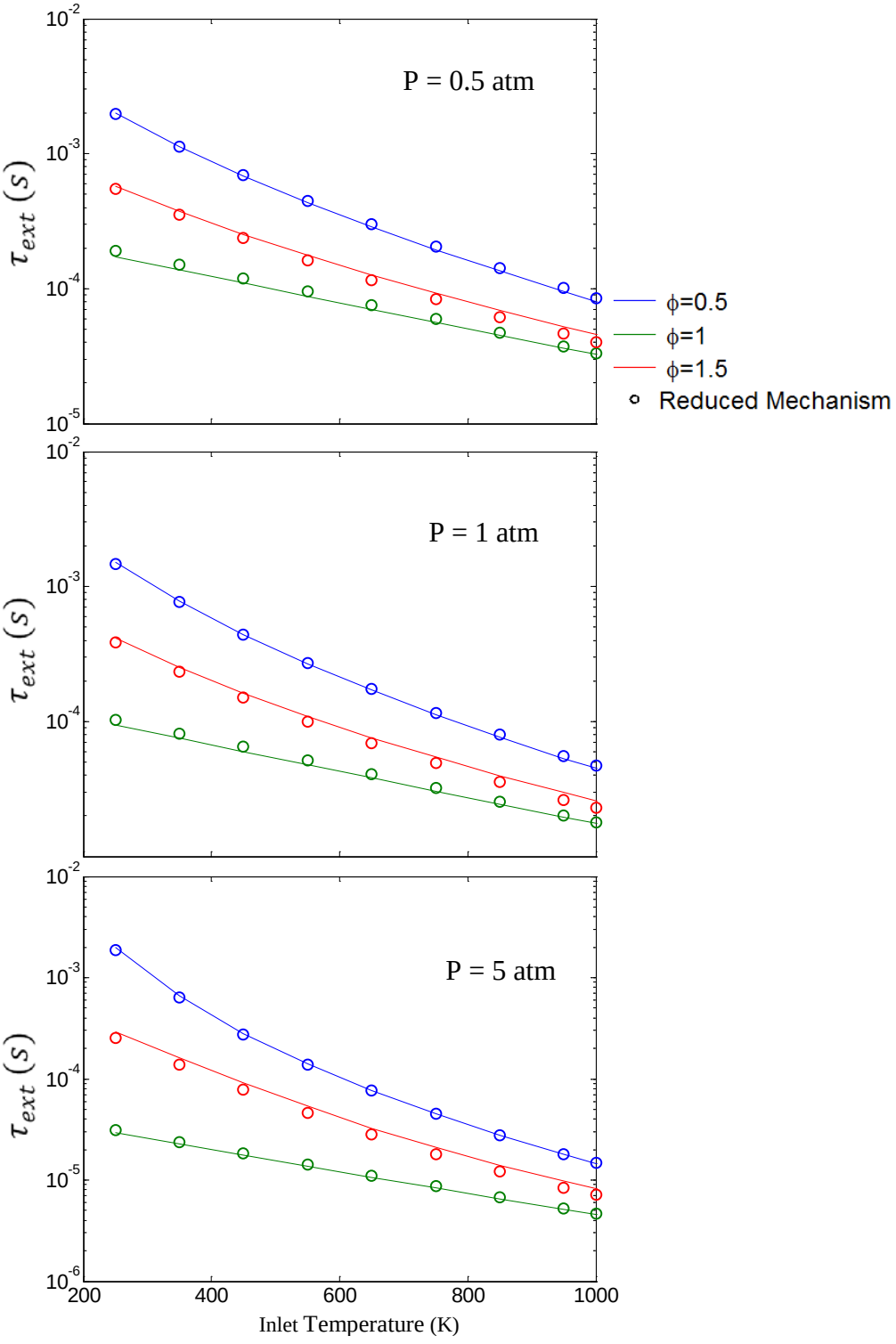

Figure 3.4 Extinction residence time in a PSR for POSF 10325 as function of inlet temperature for different equivalence ratios and pressures. Lines: detailed/lumped mechanism, symbols: reduced mechanism.

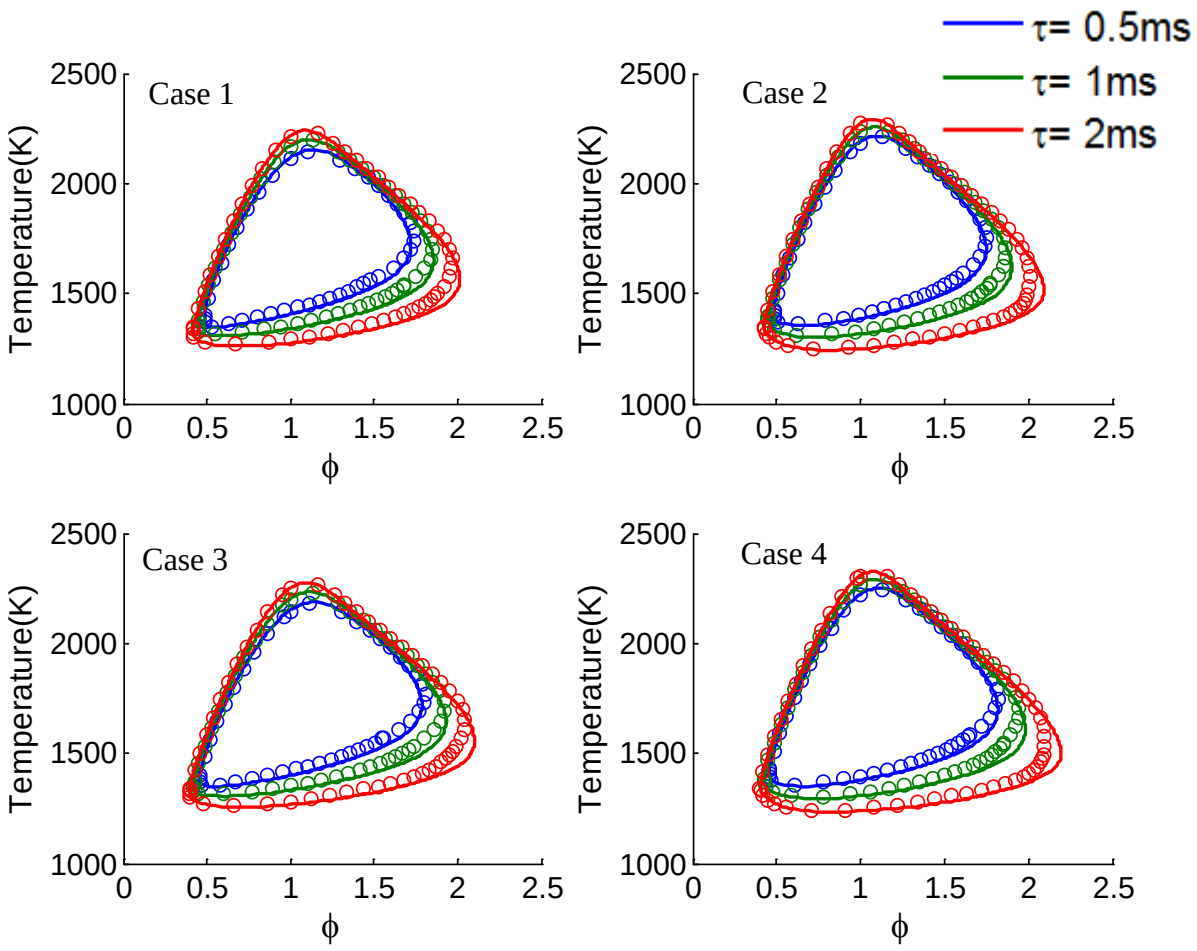

Figure 3.5 Temperature of PSR as function of equivalence ratio for reduced and detailed mechanism of n-dodecane at different conditions. Refer to Table 3.1 for case number definition. Lines: detailed mechanism, symbols: reduced mechanism.

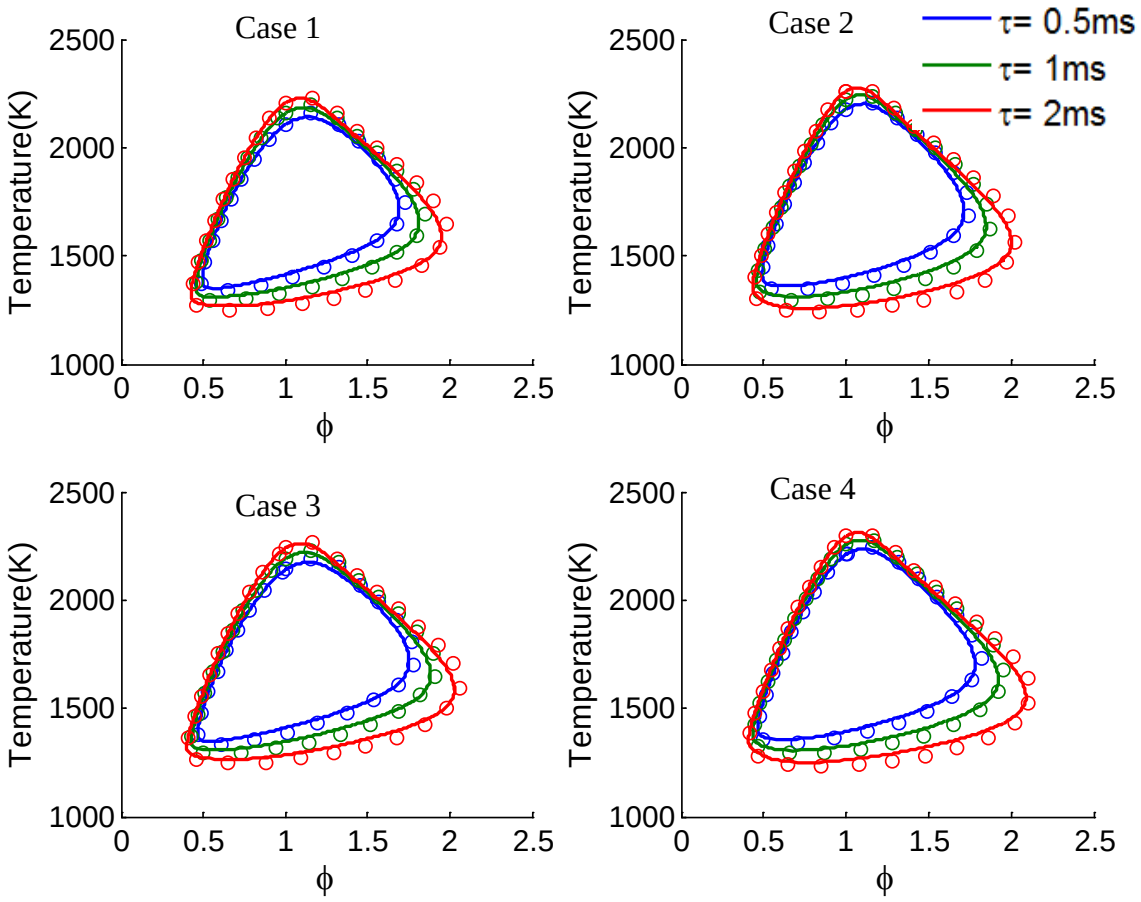

Figure 3.6 Temperature of PSR as function of equivalence ratio for reduced and detailed mechanism of POSF10325 at different conditions. Refer to Table 3.1 for case number definition. Lines: detailed mechanism, symbols: reduced mechanism.

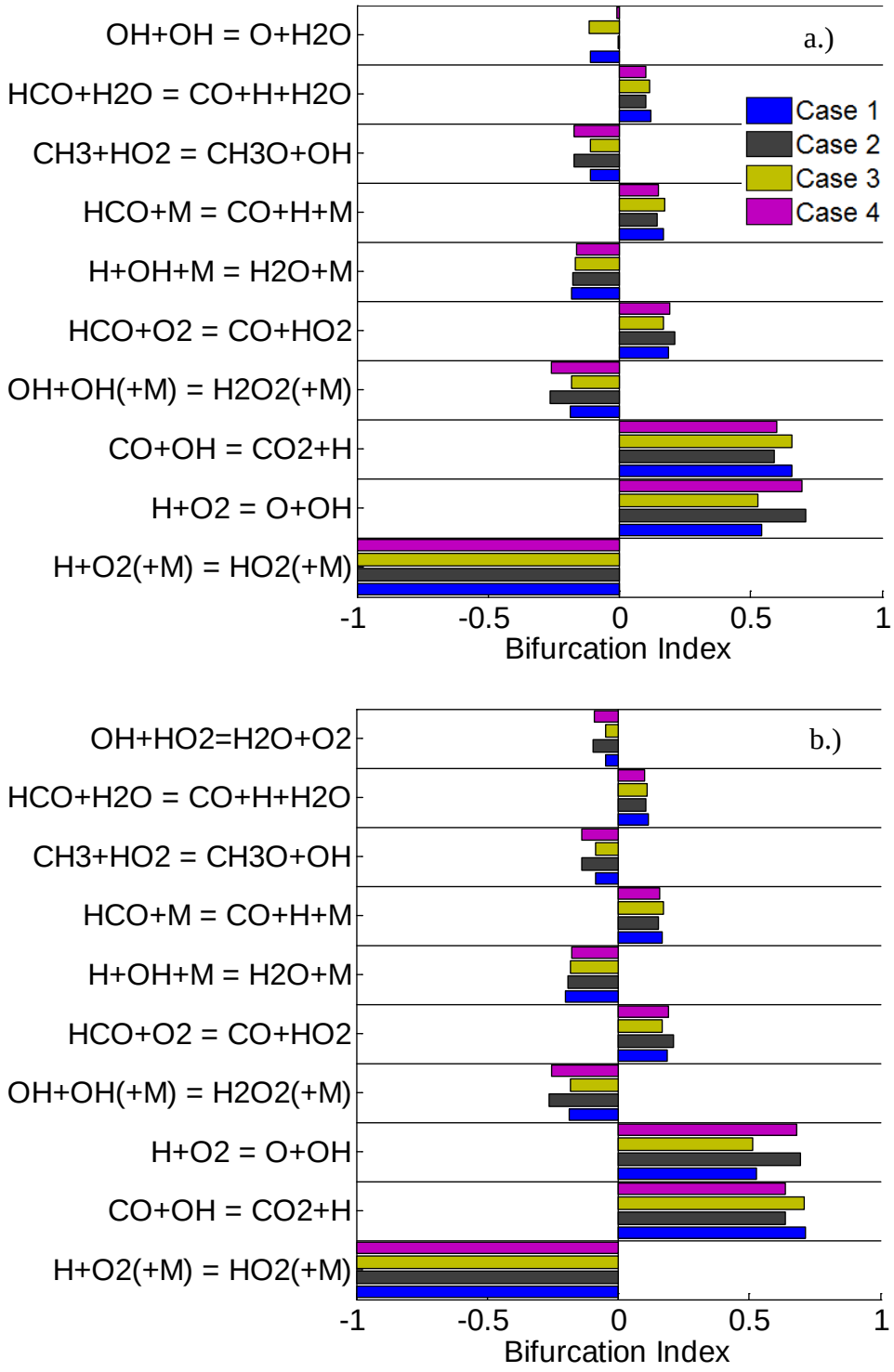

Figure 3.7 Bifurcation Index of important reactions at LBO for a. n-dodecane and b) POSF10264. Bar colors represent different conditions of the PSR referenced in Table 3.1, residence time of the reactor is $\tau = 1$ ms.

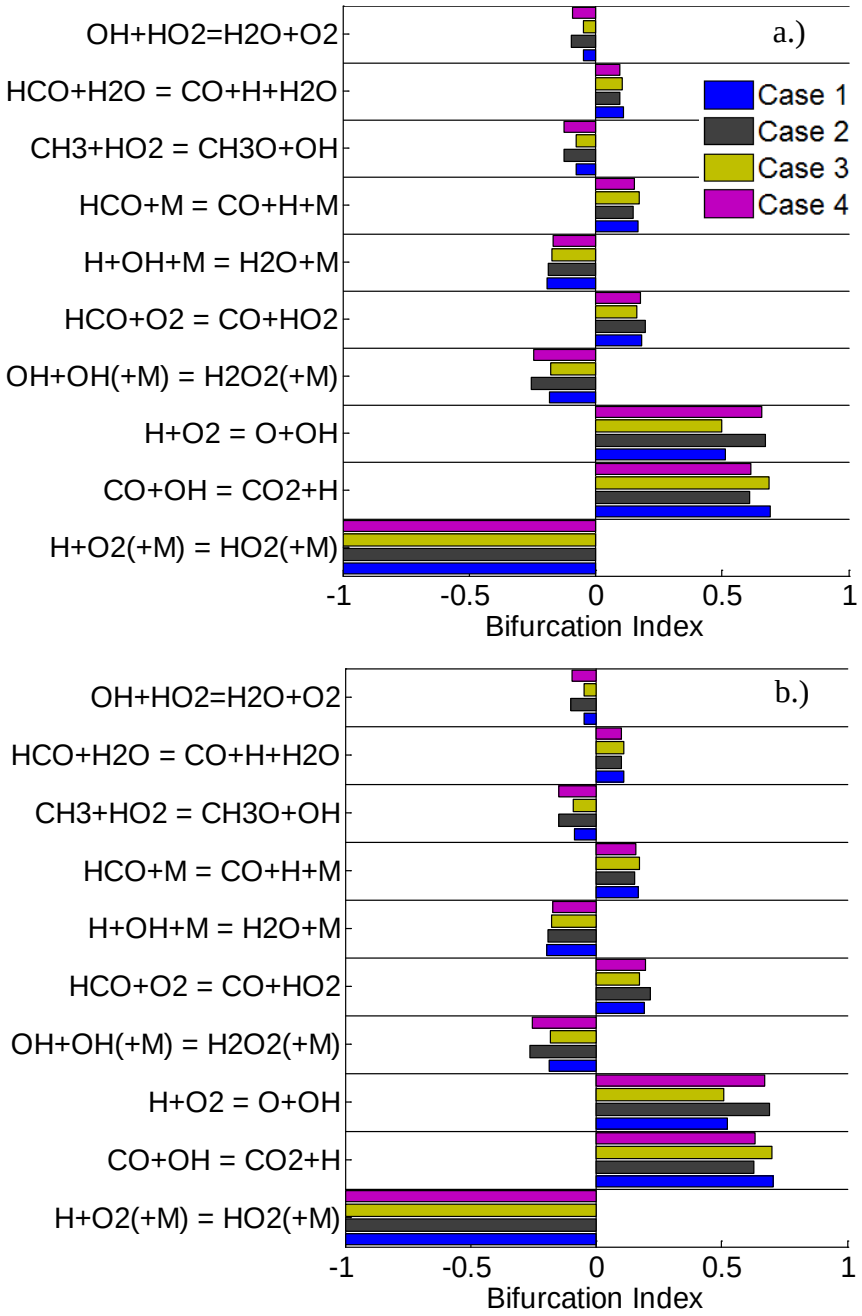

Figure 3.8 Bifurcation Index of important reactions at LBO for a) POSF10325 and b) POSF10289. Bar colors represent different conditions of the PSR referenced in Table 3.1, residence time of the reactor is $\tau = 1$ ms.

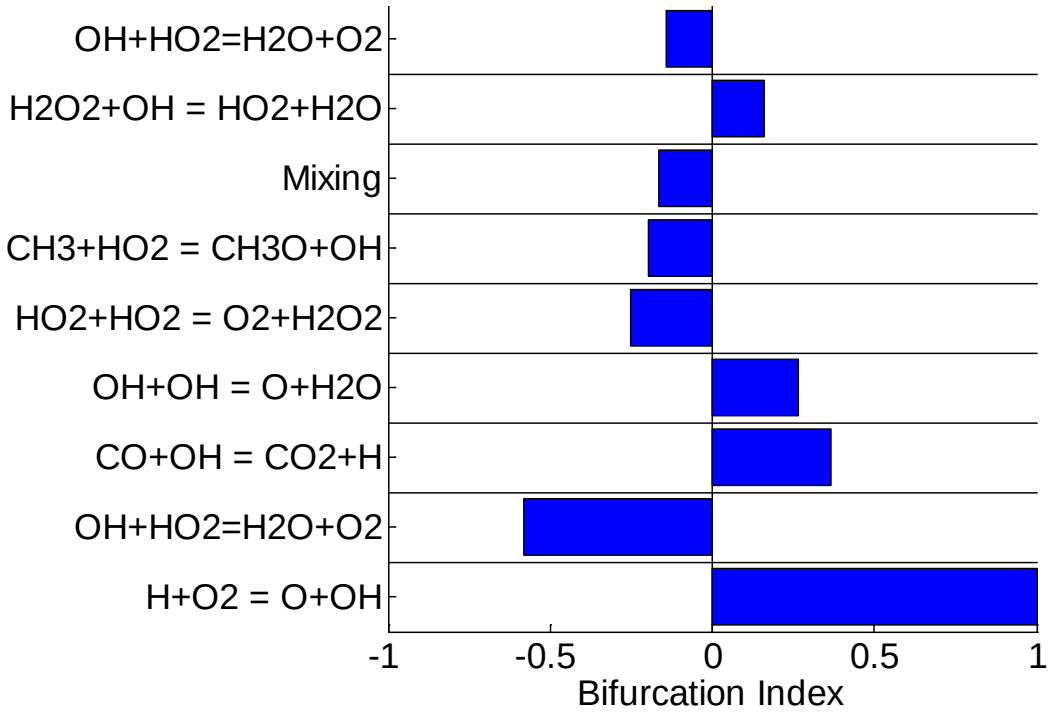

Figure 3.9 Bifurcation Index of important reactions at LBO of PSR for n-dodecane at P= 30 atm, $T_0 = 450$ K, $\tau = 1$ ms.

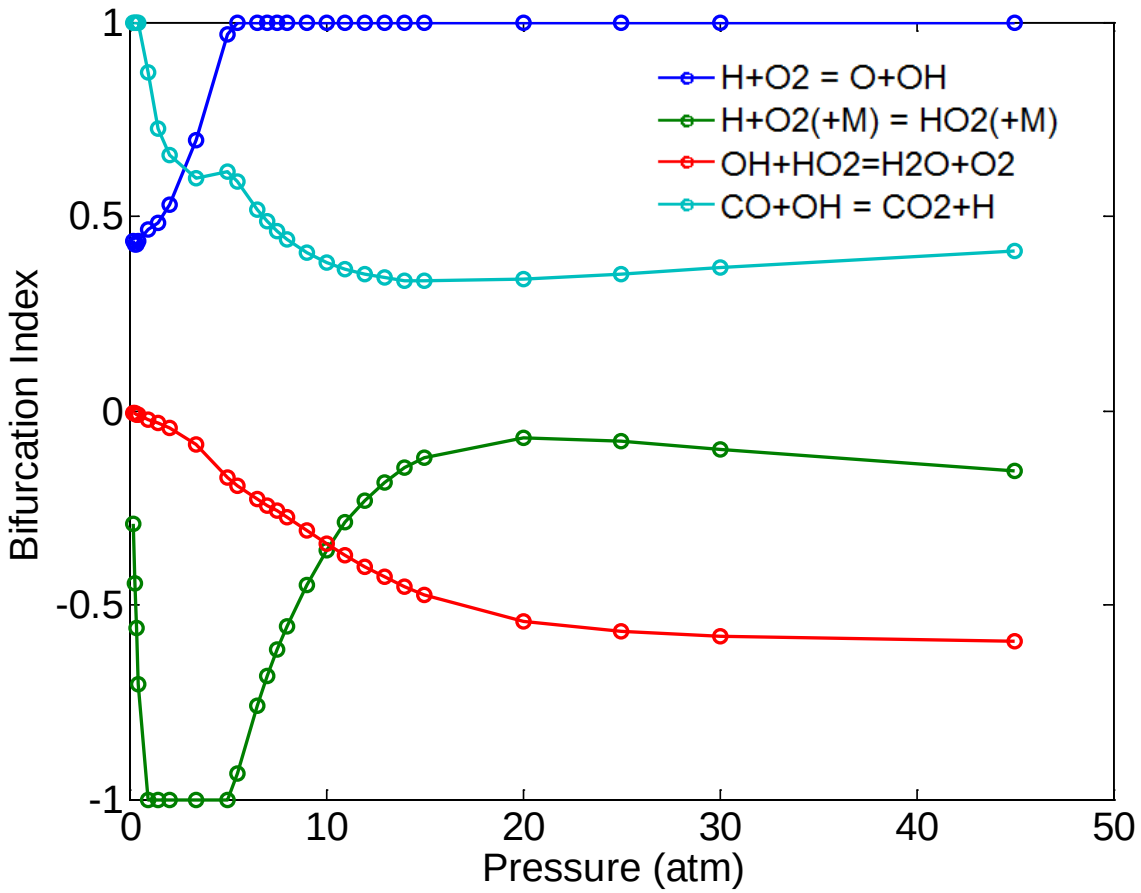

Figure 3.10 Bifurcation Index of important reactions at LBO of PSR for n-dodecane as function of pressure at $T_0 = 450\ K, \tau = 1ms$.

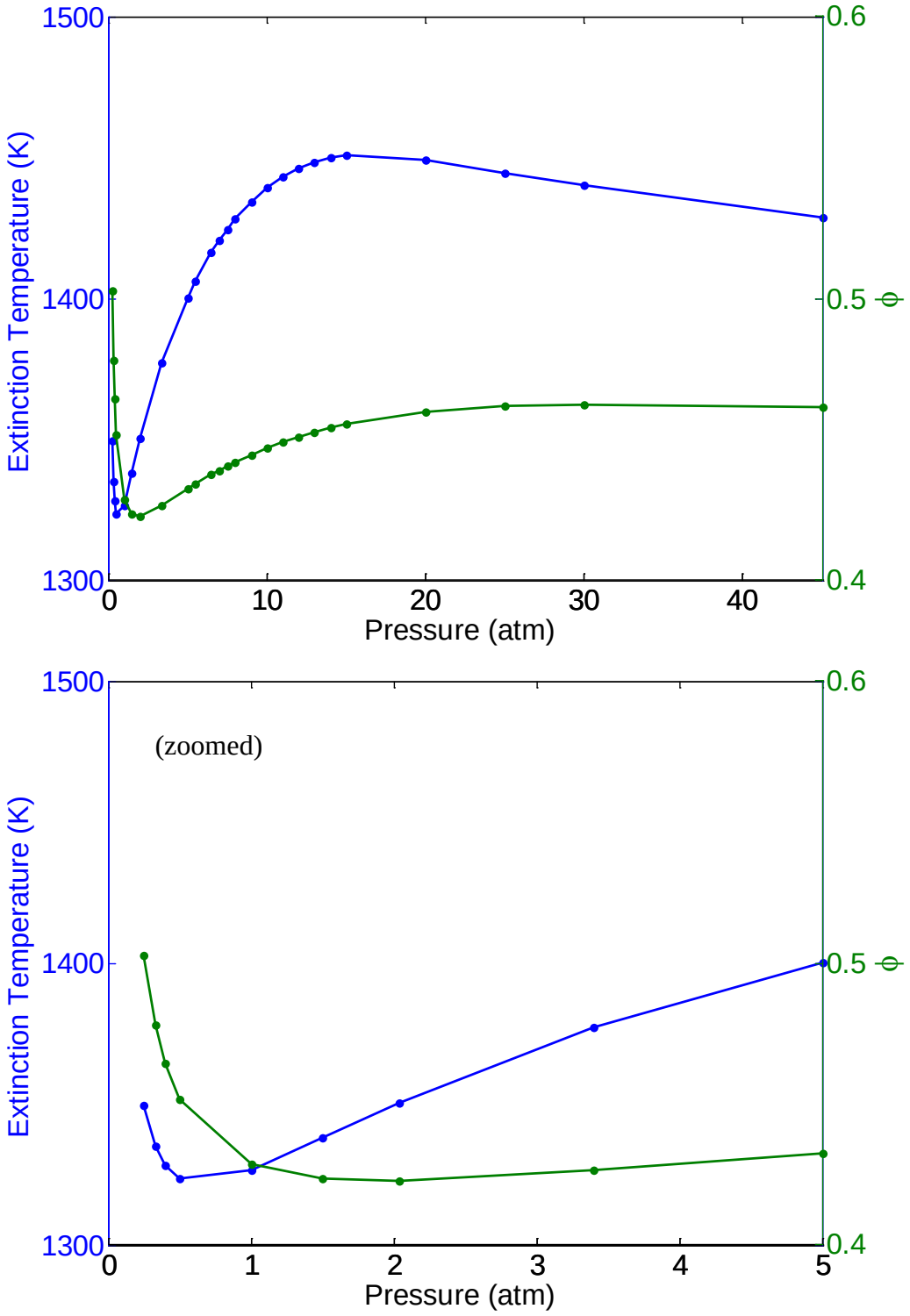

Figure 3.11 Extinction Temperature and equivalence ratio of PSR for n-dodecane/air as function of pressure at $T_0 = 450\ K$, $\tau = 1ms$. Second panel is a zoom-in of the first panel.

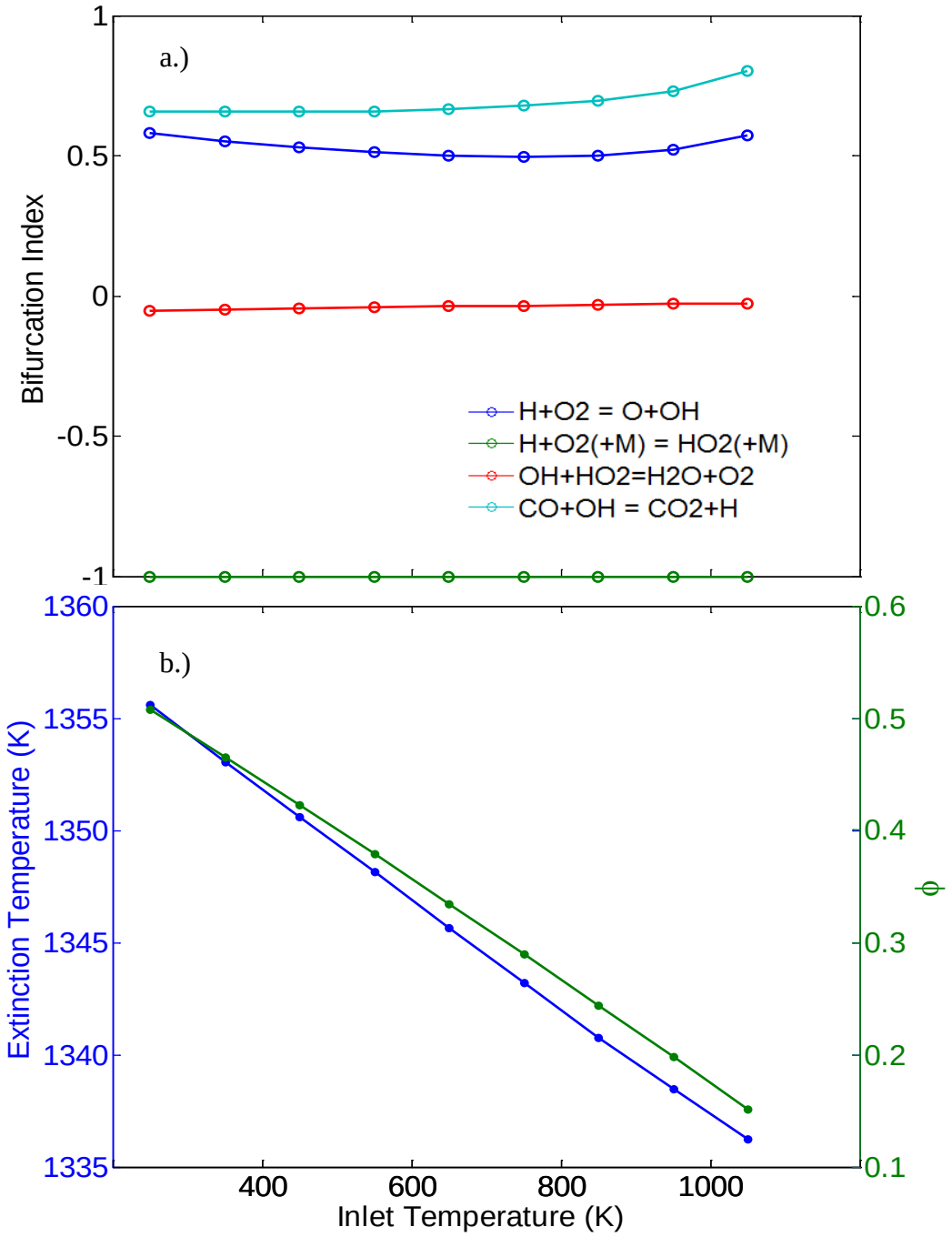

Figure 3.12 a) Bifurcation Index of important reactions at LBO of PSR for n-dodecane/air as function of inlet temperature, b) extinction temperature and equivalence ratio as function of inlet temperature for PSR conditions at $P = 2.04$ atm , $\tau = 1ms$.

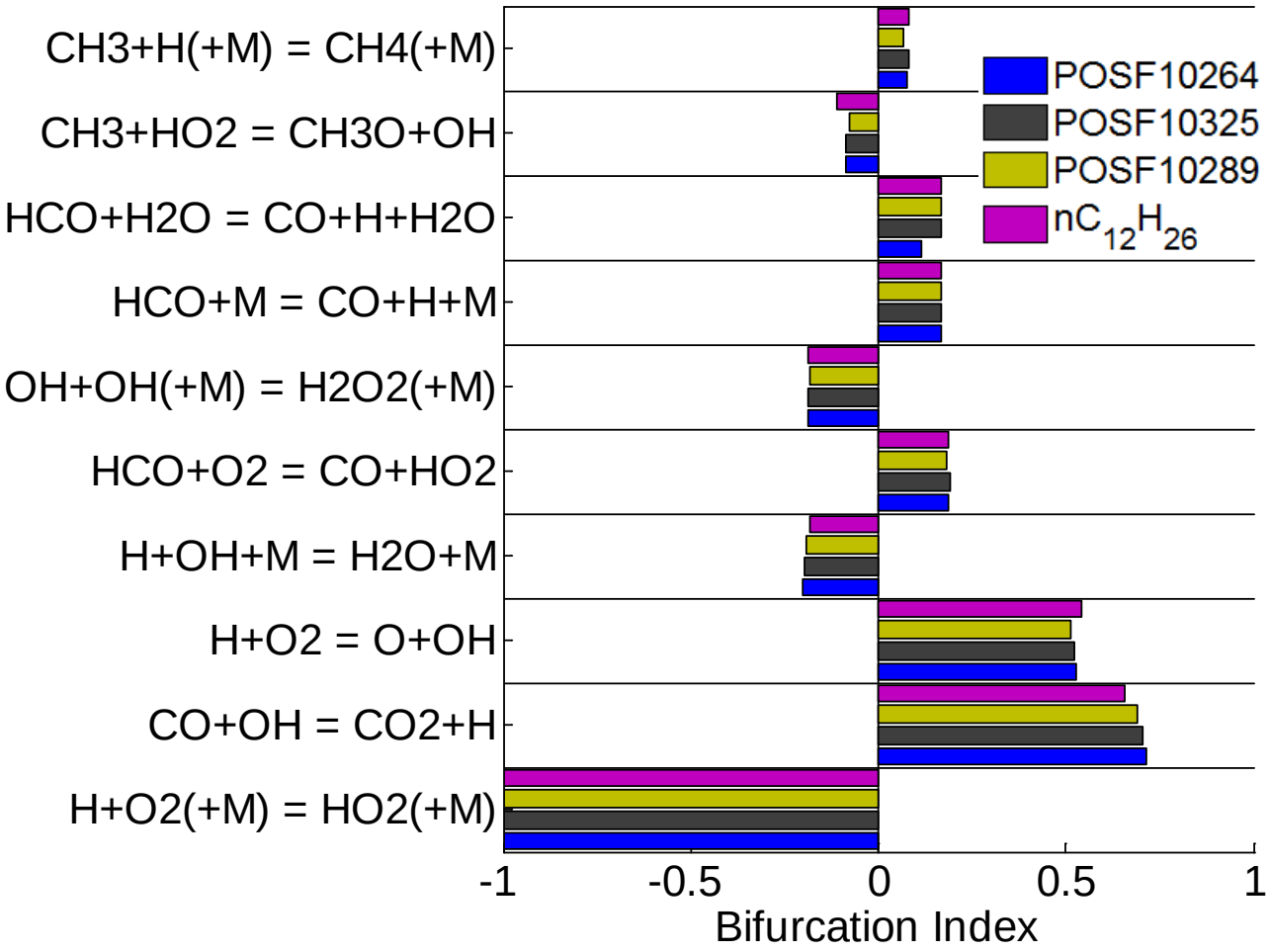

Figure 3.13 Bifurcation Index of important reactions at LBO of PSR for POSF10264, POSF10325, POSF10289, and n-dodecane at $T_0 = 394$ K, $P = 2.04$ atm, $\tau = 1$ms.

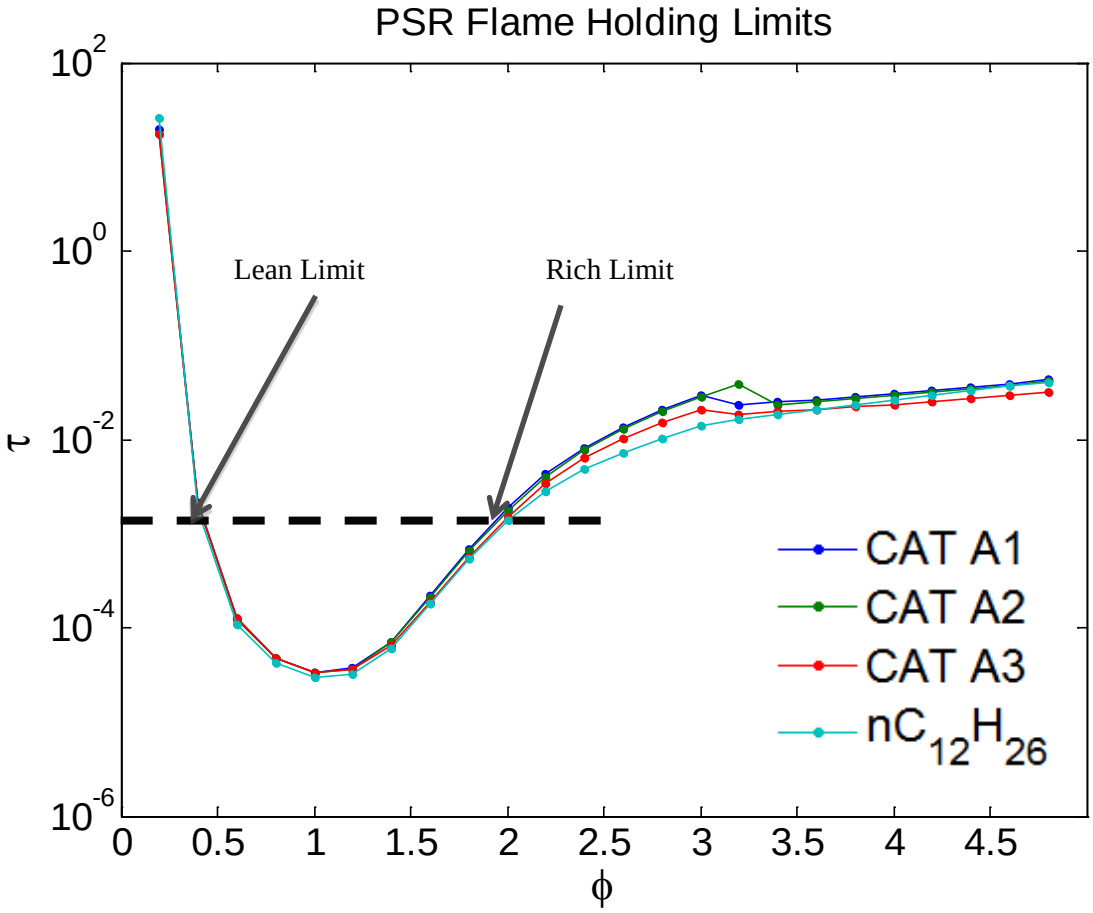

Figure 3.14 Extinction residence time of a PSR for POSF10264, POSF10325, POSF10289, and n-dodecane, respectively, at a pressure of 2.04 atm. The dashed horizontal line represents a constant residence time, its left and right intersection points with the curve designate the lean blow-out limit and rich blow-out limit, respectively.

Chapter 4. Conclusions and Future Work

In this study, reduced mechanisms of n-dodecane and POSF-10325 are investigated in PSR and are shown to predict extinction of PSR with good accuracy for equivalence ratio of 0.5-1.5, Pressure of 0.5 -5 atm, and inlet temperature of 250-1000 K. Reaction pathways of n-dodecane, POSF10264, POSF10325, and POSF10289 controlling the extinction were also investigated using bifurcation analysis and detailed mechanisms. Important extinction chemistry at LBO was found to primarily involve small molecules (e.g. H, OH, CO, HO_2). The reaction pathways at LBO were found to be sensitive to pressure that can significantly affect the HO_2 controlled chain branching pathway. Over the tested conditions, it was found that the HO_2 formation becomes less important for extinction at a pressure of 5 atm and becomes insignificant at 19 atm. Furthermore, the important reaction pathways controlling extinction were found to be insensitive to inlet temperature of PSR or to fuels types investigated in this study. The four different fuels were found to have nearly identical LBO behaviors in PSR. The chemical processes were found to contribute little to fuel sensitivity of LBO in PSR over the tested conditions, while physical properties of the fuels may play an important role in LBO of real combustors.

Future work is need to construct a universal reduced mechanism for the different jet fuels to take advantage of the shared small molecule chemistry for extinction problems. Implementation of this reduced mechanism in large scale, high

fidelity models is also required in the future to determine the differences in fuel performance caused by physical properties of the fuels.

The reaction pathway analysis at LBO using the Bifurcation Index can also be extended to more exotic fuels and smaller hyrdrocarbon fuels. This includes a more complete catalogue of fuel effects and determines if there are any additional reaction pathways that will affect the LBO performance.

Future work is required in the investigation of physical properties of fuels and the effects the individual properties have on the LBO performance. This is a challenging undertaking that would produce valuable insight on the nature of LBO and optimizing fuel composition to prevent LBO.

References

[1] U.S.Doe, “Annual Energy Outlook,” 2013.

[2] D. Wilkins, “Weaning the Navy from Foreign Oil,” *Proceedings U.S Naval Institute*, pp. 76–77, Jan-2009.

[3] X. Hui, K. Kumar, C. J. Sung, T. Edwards, and D. Gardner, “Experimental studies on the combustion characteristics of alternative jet fuels,” *Fuel*, vol. 98, pp. 176–182, 2012.

[4] K. Kumar, C. J. Sung, and X. Hui, “Laminar flame speeds and extinction limits of conventional and alternative jet fuels,” *Fuel*, vol. 90, no. 3, pp. 1004–1011, 2011.

[5] K. Kumar and C. J. Sung, “A comparative experimental study of the autoignition characteristics of alternative and conventional jet fuel/oxidizer mixtures,” *Fuel*, vol. 89, no. 10, pp. 2853–2863, 2010.

[6] a. Mzé-Ahmed, K. Hadj-Ali, P. Diévart, and P. Dagaut, “Kinetics of Oxidation of a Reformulated Jet Fuel (1-Hexanol/Jet A-1) in a Jet-Stirred Reactor: Experimental and Modeling Study,” *Combust. Sci. Technol.*, vol. 184, no. 7–8, pp. 1039–1050, 2012.

[7] D. Valco, G. Gentz, C. Allen, M. Colket, T. Edwards, S. Gowdagiri, M. a. Oehlschlaeger, E. Toulson, and T. Lee, “Autoignition behavior of synthetic alternative jet fuels: An examination of chemical composition effects on ignition delays at low to intermediate temperatures,” *Proc. Combust. Inst.*, vol. 35, no. 3, pp. 2983–2991, 2015.

[8] M. B. Colket, J. Heyne, M. Rumizen, J. T. Edwards, M. Gupta, W. M. Roquemore, J. P. Moder, J. M. Tishkoff, and C. Li, “An Overview of the National Jet Fuels Combustion Program,” in *54th AIAA Aerospace Sciences Meeting*, American Institute of Aeronautics and Astronautics, 2016.

[9] M. Gupta, M. Roquemore, and T. Edwards, “National Jet Fuels Combustion Program:Streamline ASTM International Jet Fuels Approval Process,” 2014.

[10] N. Liu, “Flame Ignition Studies of Convential and Alternative Jet Fuels and Surrogate Components,” *USC Grad. Sch. Diss.*, no. May, 2013.

[11] T. Lu and C. K. Law, “A directed relation graph method for mechanism reduction,” *Proc. Combust. Inst.*, vol. 30 I, no. 1, pp. 1333–1341, 2005.

[12] A. S. Tomlin, T. Turanyi, and M. J. Pilling, “Mathematical Tools for the Construction Investigation and Reduction of Combustion Mechanism.”

[13] X. L. Zheng, T. F. Lu, and C. K. Law, “Experimental counterflow ignition temperatures and reaction mechanisms of 1,3-butadiene,” *Proc. Combust. Inst.*, vol. 31 I, pp. 367–375, 2007.

[14] S. H. Lam and D. a. Goussis, “Understanding complex chemical kinetics with computational singular perturbation,” *Symp. Combust.*, vol. 22, no. 1, pp. 931–941, 1989.

[15] T. Lu and C. K. Law, “A criterion based on computational singular perturbation for the identification of quasi steady state species: A reduced mechanism for methane oxidation with NO chemistry,” *Combust. Flame*, vol. 154, no. 4, pp. 761–774, 2008.

[16] M. Colket and U. Technologies, “Combustion Rules and Tools for Alternative Fuels,” 2010.

[17] C. K. Law, *Combustion Physics*. New York: Cambridge University Press, 2006.

[18] Z. Luo, C. S. Yoo, E. S. Richardson, J. H. Chen, C. K. Law, and T. Lu, “Chemical explosive mode analysis for a turbulent lifted ethylene jet flame in highly-heated coflow,” *Combust. Flame*, vol. 159, no. 1, pp. 265–274, 2012.

[19] C. S. Yoo, E. S. Richardson, R. Sankaran, and J. H. Chen, “A DNS study on the stabilization mechanism of a turbulent lifted ethylene jet flame in highly-heated coflow,” *Proc. Combust. Inst.*, vol. 33, no. 1, pp. 1619–1627, 2011.

[20] T. F. Lu, C. S. Yoo, J. H. Chen, and C. K. Law, “Three-dimensional direct numerical simulation of a turbulent lifted hydrogen jet flame in heated coflow: a chemical explosive mode analysis,” *J. Fluid Mech.*, vol. 652, pp. 45–64, 2010.

[21] R. Shan, C. S. Yoo, J. H. Chen, and T. Lu, “Computational diagnostics for n-heptane flames with chemical explosive mode analysis,” *Combust. Flame*, vol. 159, no. 10, pp. 3119–3127, 2012.

[22] R. Shan and T. Lu, “Ignition and extinction in perfectly stirred reactors with detailed chemistry,” *Combust. Flame*, vol. 159, no. 6, pp. 2069–2076, 2012.

[23] R. Shan and T. Lu, “A bifurcation analysis for limit flame phenomena of DME/air in perfectly stirred reactors,” *Combust. Flame*, vol. 161, no. 7, pp. 1716–1723, 2014.

[24] D. Davis and R. D. Bowersox, “Stirred Reactor Analysis of Cavity Flame Holders for Scramjets,” *33rd AIAA/ASME/SAE/ASEE Jt. Propuls. Conf. Exhibnference Exhib*, 1997.

[25] I. R. Sigfrid, R. Whiddon, R. Collin, and J. Klingmann, “Influence of reactive species on the lean blowout limit of an industrial DLE gas turbine burner,” *Combust. Flame*, vol. 161, no. 5, pp. 1365–1373, 2014.

[26] I. Glassman and R. A. Yetter, *Combustion*. Elsevier, 2008.

[27] R. Shan, “Computational Flame Diagnostics with Bifurcation Analysis and Chemical Explosive Mode Analysis,” 2014.

[28] R. Seydel, *Practical bifurcation and stability analysis*. New York: Springer Verlag, 2010.

[29] M. R. Youssefi, “Development of Analytic Tools for Computational Flame Diagnostics Development of Analytic Tools for Computational Flame Diagnostics,” 2011.

[30] B. Sirjean, E. Dames, D. A. Sheen, and H. Wang, “Simplified Chemical Kinetic Models for High-Temperature Oxidation of C 1 to C 12 n - alkanes,” *Proc. 6th U.S Natl. Combust. Meet.*, pp. 1–7.

[31] T. Lu and C. K. Law, “Systematic approach to obtain analytic solutions of quasi steady state species in reduced mechanisms,” *J. Phys. Chem. A*, vol. 110, no. 49, pp. 13202–13208, 2006.

[32] Y. Gao, R. Shan, S. Lyra, C. Li, H. Wang, J. H. Chen, and T. Lu, “On lumped reduced reaction model for combustion of liquid fuels,” *Combustion*, vol. 163, pp. 437–446, 2016.

[33] A. Vié, B. Franzelli, Y. Gao, T. Lu, H. Wang, and M. Ihme, “Analysis of segregation and bifurcation in turbulent spray flames : A 3D counterflow configuration,” *Proc. Combust. Inst.*, vol. 35, pp. 1675–1683, 2015.

[34] Pratt & Whitney Research Development, “JTFI7A-21B TURBOFAN ENGINE SPECIFICATION,” 1967.

[35] M. Colket, S. Zeppien, M. Smooke, and K. Won-Wook, “Laminar Flame Speeds, Flammability Limits, and Flame/Reaction Zone Thicknesses for a

Surrogate Kerosene Fuel at Engine Operating Conditions," *50th AIAA Aerosp. Sci. Meet. Incl. New Horizons Forum Aerosp. Expo.*, 2012.

[36] S. Turns, *An Introduction to Combustion: Concepts and Applications w/Software*. McGraw-Hill Companies,Incorporated, 1999.